

EFFECT OF A SCANDIUM ADDITION ON ANODIZING AlMg ALLOYS

VPLIV DODATKA SKANDIJA NA ANODIZIRANJE ZLITIN AlMg

Katarina Kern¹, Janez Kovač², Marta Klanjšek Gunde³, Aleš Nagode¹,
Milan Bizjak¹, Matija Zorc¹, Borut Kosec¹, Blaž Karpe¹

¹University of Ljubljana, Faculty of Natural Sciences and Engineering, Slovenia

²Jožef Stefan Institute, Ljubljana, Slovenia

³National institute of Chemistry, Ljubljana, Slovenia

Prejem rokopisa – received: 2023-01-18; Sprejem za objavo – accepted for publication: 2023-02-10

doi:10.17222/mit.2023.755

Scandium (Sc) is known to be one of the most effective alloying elements of aluminum alloys. The only drawback is its high price, but that could change quickly due to the promising results of recent research on its extraction. However, the data on how it affects anodic oxidation are very scarce. In this research, we analyzed how a micro-addition of Sc to the AlMg alloy affects the growth mechanism and properties of the protective aluminium oxide layer depending on the anodization parameters. For comparison, alloy AA5083 with a similar magnesium content was also anodized with the same anodizing parameters. In all experiments, sulfuric acid (VI) with concentrations of 1.72 M or 2.2 M at temperatures of 21 °C or 35 °C was used as the electrolyte. Potentiostatic (18 V) and galvanostatic (20 mA/cm²) anodizing methods were applied. The results (SED-EDS) show that scandium is uniformly intercalated in the matrix of the oxide layer and decreases its resistivity, which increases the oxide growth rate during potentiostatic anodizing and decreases the pore density and pore diameters during galvanostatic anodizing. Moreover, it increases the mobility of cations through the oxide layer, thus accelerating the oxidation reaction in concentrated sulfuric acid electrolytes. On the other hand, the increased cation mobility considerably increases the sensitivity to the temperature of the electrolyte, which can change the growth mechanism of the oxide layer and thus its morphology.

Keywords: anodization, scandium microalloying, AlMgSc alloys, oxide protective layers

Skandij je eden izmed najbolj učinkovitih legirnih elementov aluminijevih zlitin. Njegova edina slabost je zelo visoka cena, kar pa se zaradi obetavnih rezultatov novejših raziskav glede njegovega načina pridobivanja hitro spreminja. Zelo malo je podatkov o tem kako vpliva na anodizacijo aluminijevih zlitin. V raziskavi so analizirali vpliv mikrolegeranja AlMg zlitine s skandijem na rast oksidne plasti med anodno oksidacijo tako v odvisnosti od časa kot tehnoloških parametrov anodne oksidacije. V vseh poskusih so za elektrolit uporabili žveplovo (VI) kislino s koncentracijama 1,72 M ali 2,2 M pri temperaturah 21 °C ali 35 °C. Uporabili so tako potenciostatično (18 V) kot galvanostatično metodo anodiziranja (20 mA/cm²). Rezultati (SEM/EDS) kažejo, da se skandij enakomerno vgrajuje v matrico oksidne plasti in zmanjša njeno upornost, kar poveča hitrost rasti oksidne plasti med potenciostatičnim anodiranjem ali zmanjša gostoto por in njihov premer med galvanostatičnim anodiziranjem. Poleg tega se poveča mobilnost kationov skozi oksidno plast in tako pospeši reakcijo oksidacije v koncentriranih elektrolitih žveplove (kislina). Po drugi strani pa se zaradi povečane mobilnosti kationov znatno poveča občutljivost na temperaturo elektrolita, kar lahko spremeni mehanizem rasti oksidne plasti, s tem pa tudi njena morfologija.

Ključne besede: anodizacija, mikrolegeranje s skandijem, zlitine AlMgSc, oksidna zaščita

1 INTRODUCTION

Anodic oxidation (anodizing) of aluminium or its alloys is an electrochemical process that produces a corrosion- and abrasion-resistant aluminium oxide (Al₂O₃) layer on the surface of a workpiece. Anodizing is usually done with direct current (DC) in an acid electrolyte. An oxide layer consists of a 10–100 μm thick porous layer with hexagonally shaped cells with a central pore perpendicular to the metal surface and a thin (several tens of nanometers) compact barrier oxide layer between the metal and the porous oxide layer (Figure 1). The resulting anodic layers are generally transparent to visible light, but various methods have also been developed to colour the anodic layer and then sealing the porous struc-

ture. The structure, mechanical properties and optical appearance of the anodized surface depend on the anodization parameters as well as on the composition of the aluminium alloy and its surface morphology.^{1–13}

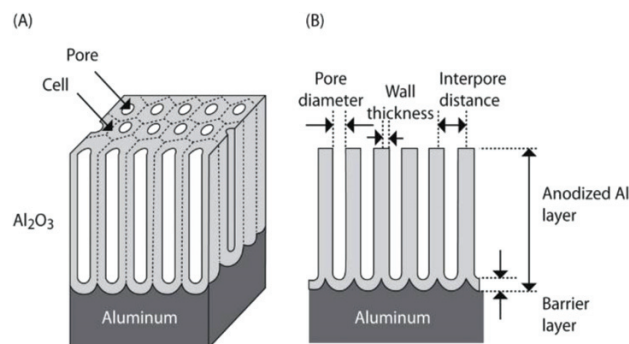


Figure 1: a) Schematic representation of the oxide layer and b) cross-section of the oxide layer²

*Corresponding author's e-mail:
blaz.karpe@ntf.uni-lj.si (Blaž Karpe)

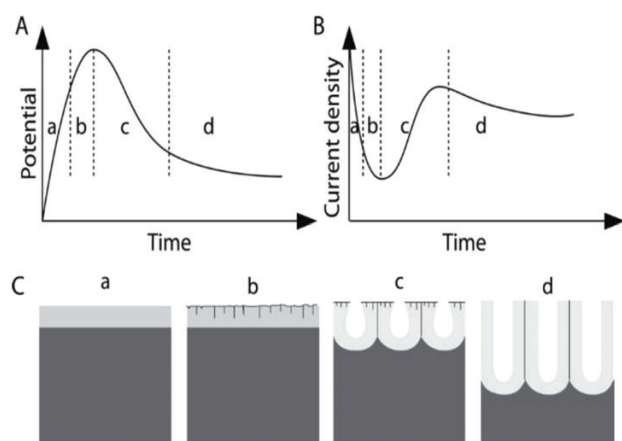


Figure 2: A) Voltage change during galvanostatic anodization, B) current density change during potentiostatic anodization, C) schematic presentation of oxide growth during the initial phases of anodization²

Figure 2 shows the change in the voltage during anodization at a constant current density (galvanostatic anodization), the change in the current density at constant voltage anodization (potentiostatic anodization), and the corresponding morphology of the oxide layer. At the beginning, a compact amorphous barrier layer is formed (range 'a'), which resembles the natural oxide layer on aluminium. After a few seconds of anodization (range 'b'), the first embryos of the pores in the barrier layer begin to form. The barrier layer thickens (to the end of range 'b'), increasing its electrical resistance. When the voltage reaches its maximum (or the current density its minimum) the barrier layer reaches its maximum thickness. In region 'c' the pores begin to deepen and increase their diameter to their final size, which leads to a decrease in the electrical resistance of the oxide layer. In region 'd', a uniform growth of the porous layer is gradually established.

The growth of a barrier and porous oxide layer on aluminium in an electric field involves the outward migration of Al^{3+} cations and the inward migration of O^{2-} or OH^- anions through the barrier oxide layer. A stable (uniform) growth of the porous oxide layer is possible only if a dynamic equilibrium is established between the growth rate of the barrier oxide layer at the metal/oxide interface and its dissolution rate at the bottom of the pores, at the oxide/electrolyte interface, which is accelerated by the electric field.

Scandium is one of the most effective precipitation strengthener, recrystallization inhibitor, and grain refiner in aluminium alloys.^{14,18} The only drawbacks include its scarcity, difficult production and the associated high price. Scandium-alloyed aluminium alloys have therefore only been used as high-priced niche products in the aerospace industry or in the sporting goods industry, such as high-performance frames for mountain bikes and baseball bats. As the new process of selective extraction of scandium from transition metals has proven successful, promising to transform the production of scandium in the

future, the interest in scandium as a microalloying element of aluminium alloys is growing in science and industry.¹⁹ One of the main advantages of scandium addition is also the improved superplasticity of some aluminium alloys, i.e., the ability of a material to exhibit highly uniform deformations by more than several hundred percent without visible necking.^{14–18} One of the superplastic aluminium alloys is AlMg microalloyed with Sc when synthesized with a suitable process. With this study, we aimed to find how a micro-addition of scandium to the AlMg alloy affects the anodization parameters, growth mechanism, and the properties of the protective aluminium oxide scale. For comparison, the AA5083 alloy with a similar magnesium content was also anodized with the same anodizing parameters.

2 EXPERIMENTAL PART

All specimens were fabricated from 1.5 mm thick cold-rolled sheets and cut into 12 mm square coupons, wet-ground with SiC abrasive paper (800, 1200, 4000), mechanically polished with diamond pastes MD-Mol 3 μm and MD-Nap 1 μm , etched in a solution of 100 g NaOH/L deionized H_2O at 60 °C for 1 min, neutralized in a solution of 6 g HNO_3 /100 mL H_2O for 4 min, rinsed in deionized water, and dried in an air flow. The chemical composition of the cold-rolled sheets used is listed in **Table 1**.

Table 1: Chemical composition of cold-rolled sheets¹⁴

El. (w/%)	AA5083	AlMgSc
Al	93.63	95.2
Mg	4.72	4.5
Si	0.25	0.008
Cr	0.14	0.0002
Mn	0.79	0.0027
Fe	0.39	0.02
Cu	0.08	0.003
Sc		0.25
Ti		0.0144

Anodizing was performed in a 100 ml anode cell at different anodization parameters:

- Potentiostatic anodization, at a constant voltage of 18 V in 1.72 M or 2.2 M H_2SO_4 acid electrolyte at 21 °C or 35 °C for up to 25 min.
- Galvanostatic anodization, at a constant current density of 20 mA/cm² in 1.72 M H_2SO_4 acid electrolyte at 21 °C for 25 min.

The electrolyte temperature during anodizing was continuously monitored with Pt100 RTD (4-wire method) and NTC 10k and kept constant by stirring and cooling with a Peltier element (QuickCool® QC-241-1.0-3.9M). The constant voltage and current density during anodization were maintained with a laboratory power supply (PSI 5080-05A Elektro-Avtomatik Gbmh).

The cross-sections of the anodized samples were analysed using a scanning electron microscope (SEM-EDS Thermo Fischer Scientific Quattro S) and Olympus BX61 optical microscope with Material Research Lab image analysis software.

3 RESULTS

3.1 Potentiostatic anodization

From the curves of the current density measurements during the initial phase of potentiostatic anodizing ($U = 18 \text{ V}$, **Figure 3**), it is evident that the kinetics of the formation of the barrier oxide layer is only slightly different for these two alloys. The main difference lies in the maximum current density i_{max} and the current density during the stationary growth phase of the porous layer, which are almost twice as large for alloy AlMgSc, result-

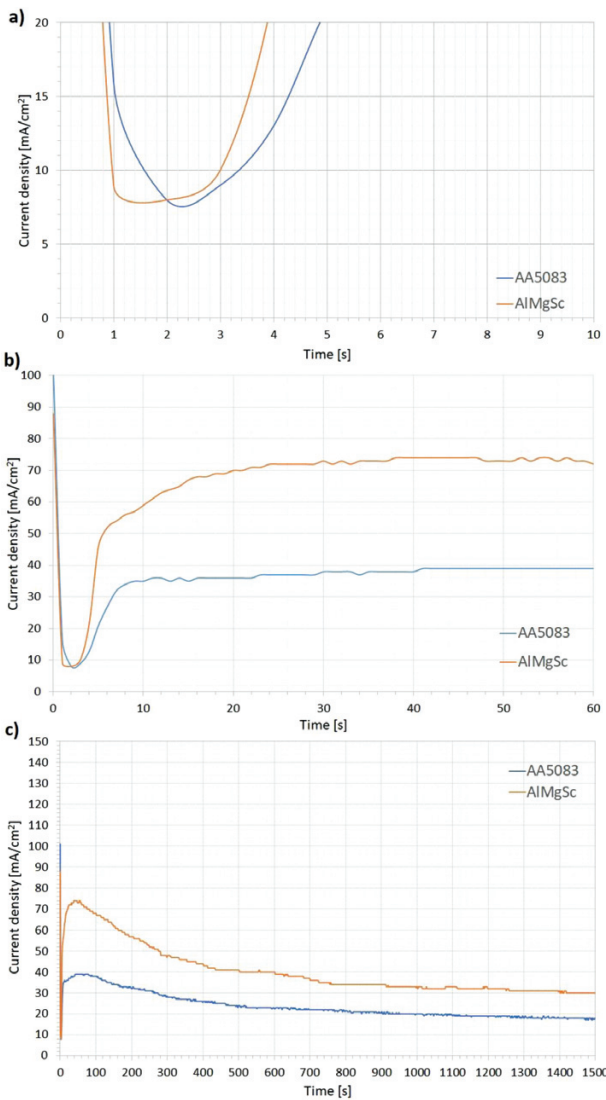


Figure 3: Current density change during anodization of AA5083 and AlMgSc aluminium alloy: a) initial phase (10 s); b) first (60 s) and c) steady state phase of anodization (25 min); a voltage of 18 V, electrolyte 1.72 M H₂SO₄, $T_{\text{el.}} = 21 \text{ }^\circ\text{C}$

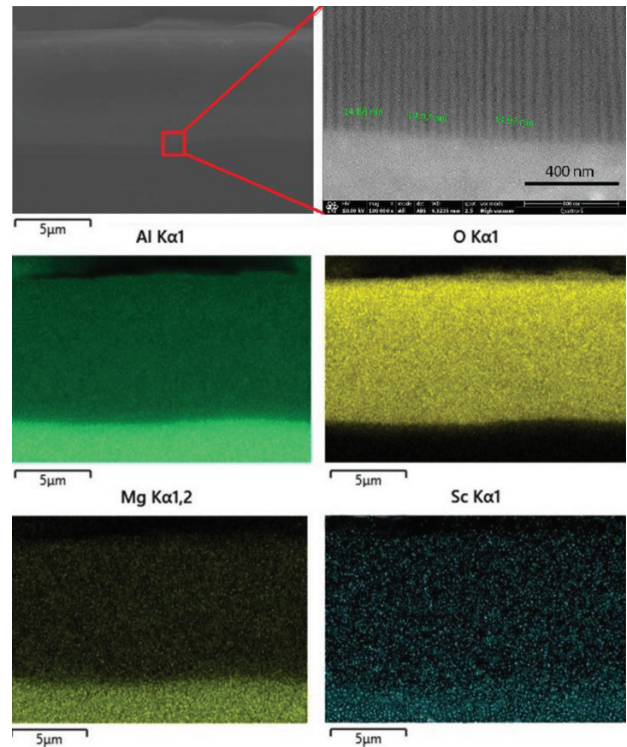


Figure 4: Specific distribution of elements (EDS mapping) in the oxide layer formed on the AlMgSc sample. An anodization time of 25 min, voltage of 18 V, electrolyte 1.72 M H₂SO₄, $T_{\text{el.}} = 21 \text{ }^\circ\text{C}$

ing in a much thicker oxide layer. The average thickness of the oxide layers after 25 min of anodization at a constant voltage of 18 V was 50 μm for AlMgSc and 25 μm for AA5083.

Figure 4 shows the specific distribution of elements (EDS mapping) in the cross-section of the oxide layer. In addition to Al, O and Mg, Sc was found to be uniformly distributed in the anodic oxide layer. Parallel pores running perpendicular to the substrate surface, 14–16 nm in diameter, can be seen at a higher magnification in the upper right micrograph.

A comparison of the pore fractions and pore diameters, measured on the free surface of the oxide layer of the two alloys, is shown in **Table 2**. While the thickness of the oxide layer varies by a factor of 2, the difference in the proportion of the pores and their diameter is practically negligible.

Table 2: Pore fractions and their diameters, measured on the free surface of the oxide layer on AA5083 and AlMgSc alloys, anodization time of 25 min, voltage of 18 V, electrolyte 1.72 M H₂SO₄, $T_{\text{el.}} = 21 \text{ }^\circ\text{C}$

Alloy	Pore fraction (%)	Pore diameter (nm)	Oxide layer thickness (μm)
AA5083	9.31	15 ± 1.7	25
AlMgSc	7.78	15.8 ± 0.9	50

3.2 Galvanostatic anodization

The curves of the voltage change (**Figure 5**) during the initial phase of galvanostatic anodization (20 mA/cm²)

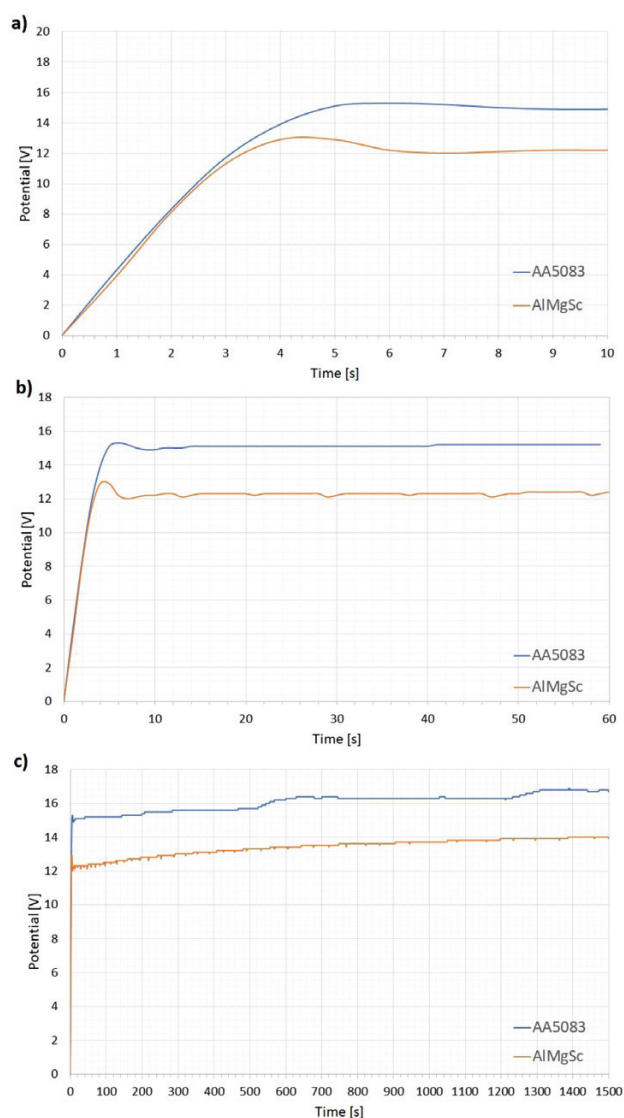


Figure 5: Voltage change during galvanostatic anodization of AA5083 and AlMgSc alloys: a) initial stage, b) after 60 s and c) steady state phase of anodization (25 min); a current density of 20 mA/cm², electrolyte 1.72 M H₂SO₄, T_{el} = 21 °C

show a similar trend of the oxide layer growth as the curves of the current density change during potentiostatic anodization. Distinctive voltages U_{max} and U_s are higher for the AA5083 alloy, indicating a higher resistance of the porous oxide layer on the AA5083 alloy. On the other hand, the thickness of the oxide layers is practically the same for both alloys, indicating that the current density determines the thickening of the oxide layer, while the voltage is related to the pore diameter and density (Table 3, Figure 6).

3.3 Electrolyte temperature effect

With an increase in the electrolyte temperature from 21 to 35 °C, the current densities i_{min} , i_{max} and i_s increase

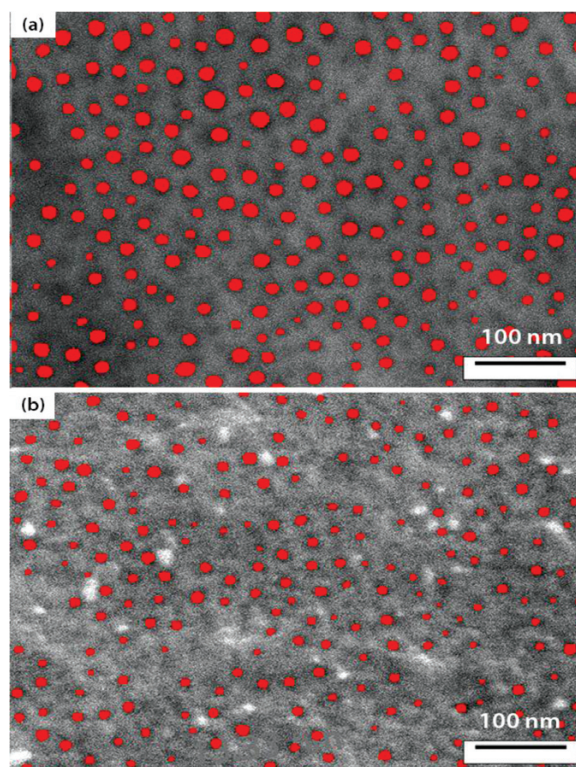


Figure 6: Pores (coloured in red) in the oxide layer (free surface): a) AA5083, b) AlMgSc; anodization time of 25 min, current density of 20 mA/cm², electrolyte 1.72 M H₂SO₄, T_{el} = 21 °C

Table 3: Pore fractions and their diameters measured on the free surface of the oxide layer on AA5083 and AlMgSc alloys, anodization time of 25 min, current density of 20 mA/cm², electrolyte 1.72 M H₂SO₄, T_{el} = 21 °C

Alloy	Pore fraction (%)	Pore diameter (nm)	Oxide layer thickness (μm)
AA5083	12.03	18.9 ± 0.4	21.5
AlMgSc	6.03	15.8 ± 1	22

significantly (Figure 8), while the barrier layer growth time and pore formation time shorten for both alloys. Despite much higher current densities, the thickness of the oxide layer increases only slightly for alloy AA5083 (from 25 μm to 29 μm), while it decreases by half for alloy AlMgSc (from 53 μm to 24 μm). The average pore diameter increases significantly, while the pore density decreases for both alloys. In addition, the mechanism of the oxide growth changes. Most of the free surface of both alloys is covered with a "bird's nest" oxide structure (Figure 7, Table 4).²⁰

3.4 Anodization in 2.2 M H₂SO₄ electrolyte at 21 °C and constant voltage

A comparison of the current density measurements during potentiostatic anodizing ($U = 18$ V) in 1.72 M and 2.2 M H₂SO₄ electrolytes shows that the maximum current density i_{max} for both alloys increases significantly in the concentrated electrolyte, while the current density

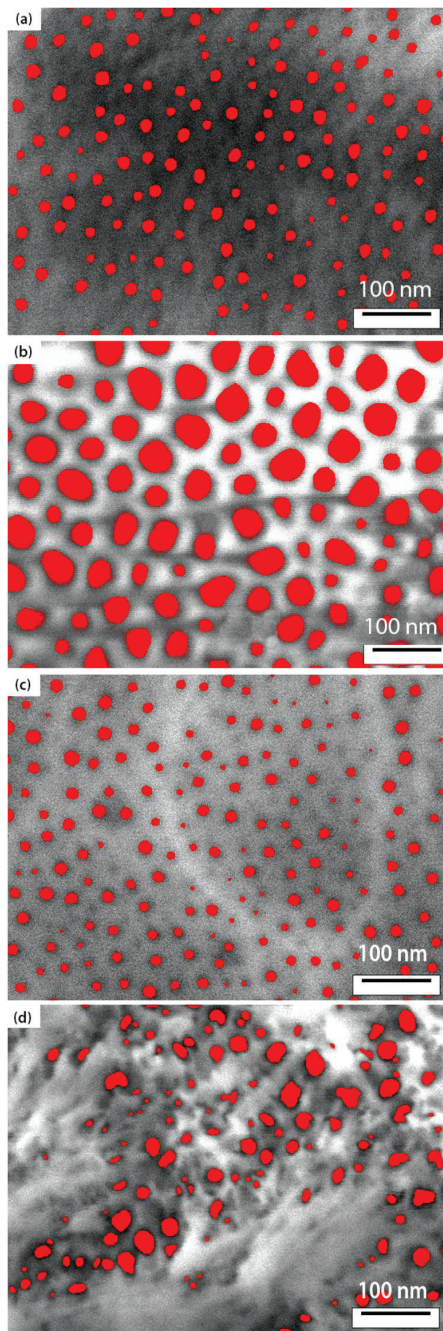


Figure 7: Pores (coloured in red) in the oxide layer (free surface) of the AA5083 alloy: a) $T_{el.} = 21\text{ }^{\circ}\text{C}$, b) $T_{el.} = 35\text{ }^{\circ}\text{C}$; and of AlMgSc: c) $T_{el.} = 21\text{ }^{\circ}\text{C}$, d) $T_{el.} = 35\text{ }^{\circ}\text{C}$; an anodization time of 25 min, voltage of 18 V, electrolyte 1.72 M H_2SO_4

Table 4: Comparison of pore densities, proportions and diameters for the oxide layers on AA5083 and AlMgSc alloys after anodizing in electrolyte 1.72 M H_2SO_4 at 21 °C or 35 °C; an anodization time of 25 min, voltage of 18 V

Alloy	El. temp. (°C)	Pore fraction (%)	Pore diameter (nm)	Oxide layer thickness (µm)
AA5083	21	9.31	15 ± 1.7	25
	35	27.42	48.4 ± 1.7	29
AlMgSc	21	7.78	15.8 ± 0.9	53
	35	8.08	/	24

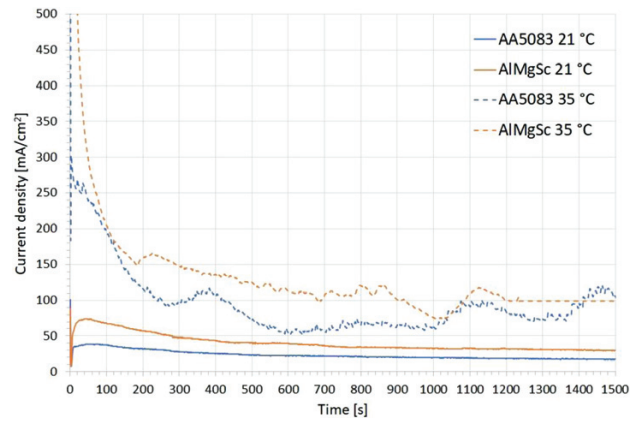


Figure 8: Current density change during potentiostatic anodization of AA5083 and AlMgSc alloys at 21 °C and 35 °C, 1.72 M H_2SO_4 electrolyte, a voltage of 18 V

in the stationary phase i_s increases only for alloy AlMgSc (**Figure 10**). The average thickness of the oxide layer after 25 min of anodization in 2.2 M H_2SO_4 is 81 µm for AlMgSc and 31 µm for AA5083 (**Figure 9**).

From the images of the free surfaces of the oxide layers formed after 25 min, it can be seen that the pore diameter increased with the increasing electrolyte concentration, especially in the case of alloy AlMgSc (**Table 5**).

Table 5: Pore diameters, density and proportions of the oxide layers on AA5083 and AlMgSc alloys; an anodization time of 25 min, voltage of 18 V, $T_{el.} = 21\text{ }^{\circ}\text{C}$

Alloy	El. conc. H_2SO_4	Pore fraction (%)	Pore diameter (nm)	Oxide layer thickness (µm)
AA5083	1.72 M	9.31	15 ± 1.7	25
	2.2 M	10.88	17.5 ± 0.2	31
AlMgSc	1.72 M	7.78	15.8 ± 0.9	53
	2.2 M	13.92	17.6 ± 1.3	81

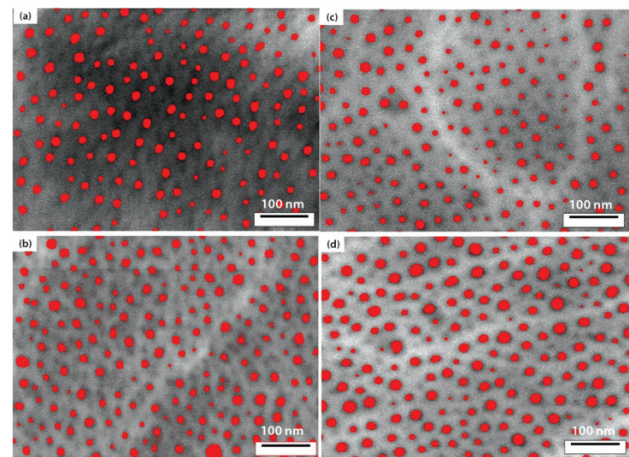


Figure 9: Pores (coloured in red) measured on the free surface of the oxide layer after anodization in electrolytes with different concentrations: a) AA5083, 1.72 M H_2SO_4 , b) AA5083, 2.2 M H_2SO_4 , c) AlMgSc, 1.72 M H_2SO_4 , d) AlMgSc, 2.2 M H_2SO_4 ; an anodization time of 25 min, voltage of 18 V, $T_{el.} = 21\text{ }^{\circ}\text{C}$

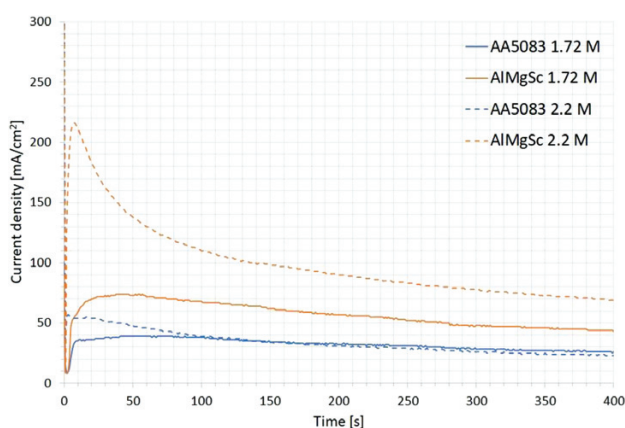


Figure 10: Current density change during anodization in 1.72 M and 2.2 M H_2SO_4 electrolytes for AA5083 and AlMgSc alloys; a voltage of 18 V, $T_{\text{el.}} = 21\text{ }^\circ\text{C}$

4 DISCUSSION

The electrical parameters of anodization (voltage and current density) are inherently related to the resistance of the growing oxide layer. If we maintain one electrical parameter constant, the value of the other depends on how the growing oxide adapts (pore density and pore diameter), which in turn depends on the chemical nature (alloying elements) as well as the processing history of the alloy to be anodized (microstructure, intermetallic phases on the surface). In addition, the value of a measured electrical parameter also depends on how the resulting oxide reacts with the electrolyte under certain conditions (type, concentration and temperature of the electrolyte). Predicting how a particular alloy will behave during anodizing is therefore extremely difficult without trial and error testing. The current density determines the thickness of the oxide layer, as it indicates how many metal anions have reacted with the cations of the electrolyte on one unit of the workpiece surface. The higher the current density, the faster is the oxide growth. However, strictly speaking, this is true only if an oxidation reaction occurs at the metal/oxide interface and the metal anions are not ejected into the electrolyte or the rate of chemical dissolution of the oxide at the oxide/electrolyte interface does not become a dominant factor.

Anodizing the same alloy at different constant voltages also affects the thickness of the barrier layer and the pore diameter of the porous layer (both of which increase with the increasing voltage). The temperature of the electrolyte has a large effect on the structure of the oxide layer as well as on the kinetics and mechanism of the growth itself. The pore diameter increases significantly even with a small increase in the temperature of the electrolyte, which is due to thermally enhanced dissolution of the pore interior supported by the electric field. At a certain temperature of the electrolyte, the

thickening of the oxide layer stops despite a high current density, which is due to an altered growth mechanism (ejection of anions into the electrolyte) or faster dissolution of the oxide at the oxide/electrolyte interface. Increasing the sulphuric acid concentration at a given voltage increases the oxide thickness due to the increased concentration of the cations available for the oxidation reaction and simultaneously increases the dissolution rate of the pore interior, increasing the pore diameter. At a certain concentration threshold, dissolution predominates and the stable oxide growth is interrupted.

Scandium has a lower Gibbs free energy of the oxide formation per equivalent ($\Delta G/n$) and a lower ionization energy than aluminium, and therefore exhibits preferential oxidation and faster cation mobility in the oxide layer, resulting in a higher current density during constant-voltage anodization or a lower voltage required to keep the current density constant during galvanostatic anodization. Scandium binds uniformly with the alumina matrix and decreases its resistivity, which in turn increases the growth rate during potentiostatic anodization or decreases the pore density and pore diameter during galvanostatic anodization. Scandium also increases the mobility of cations through the oxide layer, thus accelerating the oxidation reaction in concentrated sulphuric acid electrolytes. On the other hand, it significantly increases the sensitivity to electrolyte temperature due to the increased mobility of ions. Even small variations in electrolyte temperature can have a large effect on the oxide growth.

5 CONCLUSIONS

Alloy AlMg microalloyed with scandium is suitable for anodizing and requires a shorter anodizing time (at a constant current density) for the same oxide layer thickness as alloy AA5083, which is generally considered suitable for anodizing. The only parameter that must be carefully controlled is the electrolyte temperature, which must be kept constantly below room temperature. This is because the incorporation of Sc into the porous oxide layer increases the mobility of cations through the oxide layer, which at a certain electrolyte temperature can alter the growth mechanism by ejecting anions into the electrolyte instead of thickening the oxide layer at the metal/oxide interface.

6 REFERENCES

- ¹ H. Dong, Surface engineering of light alloys: aluminium, magnesium and titanium alloys, [s. l.], Woodhead Publishing Limited, 2010, 662
- ² A. Eftekhari, Nanostructured Materials in Electrochemistry, Wiley-VCH, Weinheim 2008, 489
- ³ J. Hirsch, T. Al-Samman, Superior light metals by texture engineering: Optimized aluminium and magnesium alloys for automotive applications, Acta Materialia, 61 (2013), 818–843, doi:10.1016/j.actamat.2012.10.044
- ⁴ W. S. Miller, L. Zhuang, J. Bottema, A. J. Wittebrood, P. De Smet, A. Haszler, A. Vierghe, Recent development in aluminium alloys

- for the automotive industry, *Materials Science and Engineering*, A280 (2000), 37–49, doi:10.1016/S0921-5093(99)00653-X
- ⁵ X. Zhang, Y. Chen, J. Hu, Recent advances in the development of aerospace materials, *Progress in Aerospace Sciences*, 97 (2018), 22–34, doi:10.1016/j.paerosci.2018.01.001
- ⁶ G. E. Totten, S. D. Mac Kenzie, *Handbook of Aluminum: Volume 2: Alloy Production and Materials Manufacturing*, CRC Press, New York 2003, 736
- ⁷ A. Røyset, T. Aukrust, B. Holme, J. E. Lein, O. Lunder, T. Kolås, Visual Appearance Characteristics of Industrial Aluminium Surfaces, *Materials Today: Proceedings*, 2 (2005) 10, Part A, 4882–4889, doi:10.1016/j.matpr.2015.10.041
- ⁸ S. Kawai, *Anodizing and coloring of aluminum alloys*, University of Michigan: Finishing Publications, Michigan 2001, 165
- ⁹ M. Aggerbeck et al, Appearance of anodised aluminium: Effect of alloy composition and prior surface finish, *Surface and Coatings Technology*, 24 (2014), 28–41, doi:10.1016/j.surfcoat.2014.05.047
- ¹⁰ I. Tsangaraki Kaplanoglou, Th. Dimogerontakis, Y. M. Wang, H. H. Kuo, S. Kia, Effect of alloy types on the anodizing process of aluminium, *Surface & Coating Technology*, 200 (2006), 2634–2641, doi:10.1016/j.surfcoat.2005.07.065
- ¹¹ X. Zhou, G. E. Thompson, P. Skeldon, G. C. Wood, K. Shimizu, H. Habazaki, Film formation and detachment during anodizing of Al-Mg alloys, *Corrosion Science*, 41 (1999), 1599–1613, doi:10.1016/S0010-938X(99)00007-4
- ¹² Y. Liu, P. Skeldon, G. E. Thompson, H. Habazaki, K. Shimizu, Anodic film growth on an Al–21at.%Mg alloy, *Corrosion Science*, 44 (2002), 1133–1142, doi:10.1016/S0010-938X(01)00115-9
- ¹³ A. C. Crosslanda, G. E. Thompsona, C. J. E. Smithb, H. Habazakic, K. Shimizud, P. Skeldon, Formation of manganese-rich layers during anodizing of Al-Mn alloys, *Corrosion Science*, 41 (1999), 2053–2069, doi:10.1016/S0010-938X(99)00025-6
- ¹⁴ A. Smolej, B. Skaza, E. Slaček, Superplasticity of the 5083 aluminium alloy with the addition of scandium, *Materials and Technology*, 43 (2009) 6, 299–302
- ¹⁵ K. A. Padmanabhan, R. A. Vasin, F. U. Enikeev, *Superplastic flow: Phenomenology and mechanics*, Springer, Berlin 2001
- ¹⁶ V. Luo, C. Miller, G. Luckey, P. Friedman, Y. Peng, On practical forming limits in superplastic forming on aluminium sheet, *Journal of Materials Engineering and Performance*, 16 (2007) 3, 274–238, doi:10.1007/s11665-007-9048-9
- ¹⁷ A. Smolej, Razvoj sodobnih zlitin aluminija, Kovine, zlitine, tehnologije, 26 (1992), 172–177, URN:NBN:SI:DOC-EOL4OQV4
- ¹⁸ C. Xu, W. Xiao, S. Hanada, H. Yamagata, C. Ma, The effect of scandium addition on microstructure and mechanical properties of Al–Si–Mg alloy: A multi-refinement modifier, *Materials Characterization*, 110 (2015), 160–169, doi:10.1016/j.matchar.2015.10.030
- ¹⁹ W. Bensalah, M. Feki, M. Wery, H. F. Ayedi, Chemical dissolution resistance of anodic oxide layers formed on aluminum, *Transactions of Nonferrous Metals Society of China*, 21 (2011) 7, 1673–1679, doi:10.1016/S1003-6326(11)60913-8
- ²⁰ J. Ye, Q. Yin, Y. Zhou, Superhydrophilicity of anodic aluminum oxide films: From "honeycomb" to "bird's nest", *Thin Solid Films*, 517 (2009), 6012–6015, doi:10.1016/j.tsf.2009.04.042